

1. Report No. SWUTC/92/712415-1		2. Government Accession No.		3. Recipient's Catalog No.	
4. Title and Subtitle Computational Realizations of the Entropy Condition in Modeling Congested Traffic Flow				5. Report Date April 1992	
				6. Performing Organization Code	
7. Author(s) Dat D. Bui, Paul Nelson, and Srinivasa L. Narasimhan				8. Performing Organization Report No. Research Report 712415-1	
9. Performing Organization Name and Address Texas Transportation Institute Texas A&M University System College Station, Texas 77843-3135				10. Work Unit No.	
				11. Contract or Grant No. 0079	
12. Sponsoring Agency Name and Address Southwest Region University Transportation Center Texas Transportation Institute The Texas A&M University System College Station, TX 77843-3135				13. Type of Report and Period Covered Final Report April 1992	
				14. Sponsoring Agency Code	
15. Supplementary Notes Supported by a grant from the U.S. Department of Transportation, University Transportation Centers Program					
16. Abstract Existing continuum models of traffic flow tend to provide somewhat unrealistic predictions for conditions of congested flow. Previous approaches to modeling congested flow conditions are based on various types of "special treatments" at the congested freeway sections. Ansoorge (Transpn. Res. B, 24B(1990), 133-143) has suggested that such difficulties might be substantially alleviated, even for the simple conservation model of Lighthill and Whitman, if the entropy condition were incorporated into the numerical schemes. In this report the numerical aspects and effects of incorporating the entropy condition in congested traffic flow problems are discussed. Results for simple scenarios involving dissipation of traffic jams suggest that Godunov's method, which in a numerical technique that incorporates the entropy condition, is more accurate than two alternative numerical methods. Similarly, numerical results for this method, applied to simple model problems involving formation of traffic jams, appear at least as realistic as those obtained from the well-known code of FREFLO.					
NOTE: Work on this topic was initially supported by TTI and was continued by the SWUTC under Project 712415. TTI Research Report No. 1232-7 and SWUTC Report 712415-1 are being published under separate covers to satisfy the unique requirements of the two sponsoring agencies.					
17. Key Words Congested, Entropy, Continuum, Bottleneck, Simulation, Models			18. Distribution Statement No Restrictions. This document is available to the public through the National Technical Information Service 5285 Port Royal Road Springfield, Virginia 22161		
19. Security Classif. (of this report) Unclassified		20. Security Classif. (of this page) Unclassified		21. No. of Pages 41	
				22. Price	

**COMPUTATIONAL REALIZATIONS OF THE
ENTROPY CONDITION IN MODELING
CONGESTED TRAFFIC FLOW**

by

Dat D. Bui
Department of Mathematics

and

Paul Nelson and Srinivasa L. Narasimhan
Department of Computer Science

Report 712415-1

Southwest Region University Transportation Center
Texas Transportation Institute
The Texas A&M University System
College Station, TX 77843-3135

April 1992

METRIC (SI*) CONVERSION FACTORS

APPROXIMATE CONVERSIONS TO SI UNITS

Symbol	When You Know	Multiply By	To Find	Symbol
--------	---------------	-------------	---------	--------

LENGTH

in	inches	2.54	centimetres	cm
ft	feet	0.3048	metres	m
yd	yards	0.914	metres	m
mi	miles	1.61	kilometres	km

AREA

in ²	square inches	645.2	centimetres squared	cm ²
ft ²	square feet	0.0929	metres squared	m ²
yd ²	square yards	0.836	metres squared	m ²
mi ²	square miles	2.59	kilometres squared	km ²
ac	acres	0.395	hectares	ha

MASS (weight)

oz	ounces	28.35	grams	g
lb	pounds	0.454	kilograms	kg
T	short tons (2000 lb)	0.907	megagrams	Mg

VOLUME

fl oz	fluid ounces	29.57	millilitres	mL
gal	gallons	3.785	litres	L
ft ³	cubic feet	0.0328	metres cubed	m ³
yd ³	cubic yards	0.0765	metres cubed	m ³

NOTE: Volumes greater than 1000 L shall be shown in m³.

TEMPERATURE (exact)

°F	Fahrenheit temperature	5/9 (after subtracting 32)	Celsius temperature	°C
----	------------------------	----------------------------	---------------------	----

APPROXIMATE CONVERSIONS TO SI UNITS

Symbol	When You Know	Multiply By	To Find	Symbol
--------	---------------	-------------	---------	--------

LENGTH

mm	millimetres	0.039	inches	in
m	metres	3.28	feet	ft
m	metres	1.09	yards	yd
km	kilometres	0.621	miles	mi

AREA

mm ²	millimetres squared	0.0016	square inches	in ²
m ²	metres squared	10.764	square feet	ft ²
km ²	kilometres squared	0.39	square miles	mi ²
ha	hectares (10 000 m ²)	2.53	acres	ac

MASS (weight)

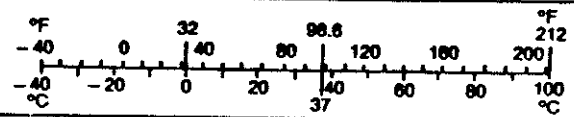
g	grams	0.0353	ounces	oz
kg	kilograms	2.205	pounds	lb
Mg	megagrams (1 000 kg)	1.103	short tons	T

VOLUME

mL	millilitres	0.034	fluid ounces	fl oz
L	litres	0.264	gallons	gal
m ³	metres cubed	35.315	cubic feet	ft ³
m ³	metres cubed	1.308	cubic yards	yd ³

TEMPERATURE (exact)

°C	Celsius temperature	9/5 (then add 32)	Fahrenheit temperature	°F
----	---------------------	-------------------	------------------------	----



These factors conform to the requirement of FHWA Order 5190.1A.

* SI is the symbol for the International System of Measurements

Abstract

Existing continuum models of traffic flow tend to provide somewhat unrealistic predictions for conditions of congested flow. Previous approaches to modeling congested flow conditions are based on various types of “special treatments” at the congested freeway sections. Ansoorge (*Transpn. Res. B*, **24B**(1990), 133-143) has suggested that such treatments might be unnecessary, and realistic predictions obtained, even for the simple conservation model of traffic flow due to Lighthill and Whitham, if the so-called “entropy condition” were incorporated into the underlying numerical schemes. (The entropy condition originally arose in computational fluid dynamics, where it serves to distinguish the physically relevant solution from nonphysical solutions of the fluid flow equations that do not satisfy the second law of thermodynamics.) In this report the numerical aspects and effects of incorporating the entropy condition into congested traffic flow problems are discussed. Results for simple scenarios involving dissipation of traffic jams suggest that Godunov’s method, which is the simplest numerical technique that incorporates the entropy condition, is more accurate than two alternate numerical methods. Similarly, numerical results for this method, applied to simple model problems involving formation of traffic jams, appear at least as realistic as those obtained from the well-known code FREFLO.

Implementation Statement

Simulating traffic in the vicinity of freeway bottlenecks is of great importance in studying and designing traffic networks. Current traffic models do not perform adequately in congested traffic conditions, which are of current special interest in studies relating to the efficient use of fuel and minimization of vehicle pollution. This effort offers promises for overcoming existing traffic modeling limitations. The information contained in this report should be useful in modeling the entropy conditions when analyzing congested vehicular traffic. The ultimate significance of this work is envisioned to be in implementation of the entropy condition in a computer code (model).

Disclaimer

The contents of this report reflect the views of the authors, who are responsible for the facts and the accuracy of the information presented herein. This document is disseminated under the sponsorship of the Department of Transportation, University Transportation Centers Program, in the interest of information exchange. The U.S. Government assumes no liability for the contents or use thereof.

Contents

1	Introduction	1
2	Traffic Flow and Weak Solutions	3
3	The Entropy Condition	6
4	A Numerical Realization of the Entropy Condition: Godunov's Method	10
5	Numerical Results for Simple Problems: Dissipation of Jams	13
6	Numerical Results for Simple Problems: Formation of Jams	16
7	Conclusions	21
	Acknowledgments	23
	References	24

List of Figures

1a	The traffic-signal release	26
1b	The moderately congested signal release	26
2	The traffic-signal release via Godunov's method	27
3	The speed-density relation	27
4	The freeway bottleneck via Godunov's method for scenario 1	28
5	The freeway bottleneck via FREFLO for scenario 1	28
6	The freeway bottleneck via Godunov's method for scenario 2	29
7	The freeway bottleneck via FREFLO for scenario 2	29

List of Tables

1	Traffic densities obtained from Godunov's method for scenario 1	30
2	Traffic densities obtained from Godunov's method for scenario 2	30
3	Traffic densities obtained from FREFLO for scenario 1	31
4	Traffic speeds obtained from FREFLO for scenario 1	31
5	Traffic in-flow rates obtained from FREFLO for scenario 1	32
6	Traffic out-flow rates obtained from FREFLO for scenario 1	32
7	Traffic densities obtained from FREFLO for scenario 2	33
8	Traffic speeds obtained from FREFLO for scenario 2	33
9	Traffic in-flow rates obtained from FREFLO for scenario 2	34
10	Traffic out-flow rates obtained from FREFLO for scenario 2	34

Chapter 1

Introduction

Precise understanding of traffic conditions during periods of congestion is a major problem in traffic engineering practice (see [2, 10-15]). Simulation models in the vicinity of freeway bottlenecks are of great importance in studying and designing traffic networks. However, simulation models based on the existing continuum models of traffic flow tend to provide somewhat unrealistic predictions, especially in either the transition region downstream of a bottleneck or the “shock” region at the maximum upstream extent of the influence of such a bottleneck. Previous approaches to modeling of congested flow conditions are based on techniques that require great care for congested flow situations. Payne [11-12] resolved this problem in his substantially developed FREFLO (a macroscopic freeway simulation) by requiring special user inputs for congested freeway sections. These include modifications to the (discontinuous) speed-density relationship or to the calibration of the dynamic interaction variables. Babcock et al. [2] suggested using a smaller discrete increment at the congested freeway sections. Their numerical experiments indicated that very small spatial steps are needed to realistically simulate congested flow conditions. Such discretizations require a substantial amount of computing time. Rathi et al. [14] addressed the problem of excessively high densities by implementing flow restrictions to congested freeway links. These modifications are applied whenever the density of the freeway section exceeds a prespecified value.

Although all these techniques offer some amelioration for congested freeway problems, they are based on “special treatments” at the congested freeway sections. Furthermore, questions remain regarding the ability of these approaches to simulate severely congested flow situations. Ansoorge [1] has suggested that such difficulties for congested flow problems might be substantially alleviated, even for the classically simple conservation model of

Lighthill and Whitham [8], if numerical methods ensuring an “entropy condition” (somewhat better known in fluid dynamics than in traffic theory) were employed; he suggested further that numerical approximations that do not satisfy such condition essentially correspond to unrealistic expectations about the anticipatory behavior of drivers at a region of rapidly varying concentration. See Chapter 3 below for a more detailed introduction to the concept of entropy condition.

The essential purpose of this report is to describe the results of a preliminary investigation of this suggestion. In more detail, the structure of this report is as follows. In Chapter 2 we introduce our notation for the classical Lighthill-Whitham model [8], discuss the need for introducing weak solutions of this conservation law, in order to have solutions of reasonable traffic-flow problems that exist for all time, and present an example (following Ansorge [1]) from the theory of traffic flow that shows such solutions introduce a new difficulty, in the form of nonuniqueness of solutions. In Chapter 3 we describe a convenient form of the entropy condition, show how it restores uniqueness, describe some specific entropy-satisfying solutions of the Lighthill-Whitham model that have particular significance in traffic-flow theory, and discuss issues relating to the fundamental meaning of the entropy condition in the context of traffic flow theory. In Chapter 4 we describe, in the context of the Lighthill-Whitham model, Godunov’s method [9] for numerical solution of scalar conservation laws; this seems to be the simplest such numerical method that admits an entropy condition, and hence it is the method that was employed for our study. Some sample numerical results, for a number of rather simple scenarios involving dissipation of traffic jams, are presented and discussed in Chapter 5. Chapter 6 contains corresponding sample numerical results for simple model problems leading to formation of jams. In addition to results from Godunov’s method, in Chapter 5 we also present, for purposes of comparison, results from other numerical methods for scalar conservation laws (the upwind and Lax-Friedrichs methods); for the problems involving jam formation (Chapter 6) we also present results from the well-known FREFLO code [11, 14], as this is a class of problems for which this benchmark code is well-known to have some difficulties [14]. In Chapter 7 we present our conclusions and related suggestions for further study.

Chapter 2

Traffic Flow and Weak Solutions

Consider the model of Lighthill and Whitham [8]

$$\frac{\partial k}{\partial t}(x, t) + \frac{\partial q}{\partial x}(x, t) = g(x, t), \quad \forall x \in I, t \geq 0, \quad (2.1)$$

where $k(x, t)$ is the traffic density, $q(x, t)$ is the traffic flow rate, $g(x, t)$ is the source term (e.g., vehicles entering or leaving the freeway), and I is the corresponding freeway segment. Often $g(x, t)$ is taken to be zero. The initial conditions

$$k(x, 0) = k_0(x), \quad x \in I, \quad (2.2)$$

are assumed to be given. We also assume that q depends explicitly on k (i.e., *fundamental diagram condition*). Thus

$$q = q(k) = kv \quad (v = v(k)), \quad (2.3)$$

where v is the traffic mean speed (and hence $v' < 0$, where primes denote derivatives of functions of a single variable). The function q is a strictly concave function, which is to say it satisfies

$$q''(k) < 0, \quad 0 < k < k_j, \quad (2.4)$$

where $k_j > 0$ is the maximum (traffic jam) density ($v(k_j) = 0$).

Consider the case that the source term (i.e., g) in (2.1) is zero. A *classical solution* of the initial-value problem (2.1)-(2.3) for the corresponding scalar conservation law (2.1) is, by definition, continuously differentiable in both x and t . Thus such a solution must satisfy

$$\frac{\partial k}{\partial t}(x, t) + q'(k) \frac{\partial k}{\partial x}(x, t) = 0, \quad \forall x \in I, t \geq 0,$$

and therefore must correspond to constant concentration along each of the family of *characteristics*

$$x = x(t) = x_0 + q'(k_0(x_0))t \quad (2.5)$$

parametrized by the initial point x_0 . Following Lighthill and Whitham [8], we shall term $q'(k)$ as the *wave velocity* at concentration k . (A solution value propagating along such a characteristic similarly could be termed a “kinematic wave.”)

It is unfortunate, but also well-known and rather easily seen (e.g., §3 of Lax [7]), that there are reasonable circumstances under which such an initial-value problem need not have a solution globally (i.e., for all $t > 0$). These correspond to situations such that different characteristics (2.5) intersect at some point (x, t) , and hence any classical solution would have contradictory values at such a point. In the Lighthill-Whitham traffic model of interest here, this will happen if the initial concentration (2.2) has a region of lower concentration (and hence higher mean speed) upstream of a region of higher concentration (and hence lower mean speed). Physically this corresponds to formation of a shock, but classical solutions must be continuous and thus cannot contain shocks. Therefore it is necessary to extend the concept of “solution,” in order to have a mathematical theory that meets the needs of traffic-flow theory.

This need is met by introducing the concept of *weak solution*. A weak solution of the problem (2.1)-(2.3) is a function $k(x, t)$, defined for $x \in I$ and $t \geq 0$, such that

$$-\int_{-\infty}^{\infty} \int_0^{\infty} [k\phi_t + q\phi_x] dt dx - \int_{-\infty}^{\infty} \phi(x, 0)k_0(x) dx = 0, \quad (2.6)$$

for all “sufficiently smooth” functions $\phi(x, t)$. (It also is necessary to specify that k satisfy the technical condition of “local integrability”; see Ref. 9 for details.) Every such weak solution that is also continuously differentiable in fact is a classical solution of (2.1)-(2.3), but there are weak solution that are not classical solutions. In particular, there are weak solutions that contain shocks, which is to say curves in the (x, t) -plane along which the solution is discontinuous. While this concept of weak solution thus remedies the deficiency of classical solutions, it also introduces a difficulty in its own right. Specifically, a given initial-value problem of the form (2.1)-(2.3) may have more than one weak solution.

We now follow Ansorge [1] (see also §4.1 of LeVeque [9]) in presenting an example from traffic-flow theory of this lack of uniqueness for weak solutions of initial-value problems of the form (2.1)-(2.3). Consider the specific Greenshields model [4] of the generic fundamental diagram (2.3)

$$q(k) = v_f \left(1 - \frac{k}{k_j}\right)k. \quad (2.7)$$

Here, $v_f = v(0)$ is the maximum (freeflow) mean traffic speed. Further consider the problem of dissolution of a traffic jam, say with initial condition

$$k_0 = \begin{cases} k_j, & \text{for } x < 0 \\ 0, & \text{for } x \geq 0. \end{cases} \quad (2.8)$$

The problem (2.1), (2.2), (2.7), and (2.8) then has the weak solutions

$$k_1(x, t) = \begin{cases} k_j & \text{for } x < -v_f t, t \geq 0. \\ k_j \frac{v_f t - x}{2v_f t} & \text{for } -v_f t \leq x < v_f t, t > 0. \\ 0 & \text{for } x \geq v_f t, t \geq 0, \end{cases} \quad (2.9)$$

and

$$k_2(x, t) = k_0(x), \quad \forall t \geq 0. \quad (2.10)$$

Thus, the question is which of these is the physically correct solution to the problem. Ansorge [1] suggested using the so-called “entropy condition” to select the (unique) weak solution that corresponds to the actual behavior of traffic. In the following section we shall first describe the form of entropy condition that is most convenient for our purposes, then show how it can be used to determine the “correct” weak solution to the above and other similar initial-value problems for the Lighthill-Whitham model, and finally we discuss the basis in traffic-flow theory for this condition.

Chapter 3

The Entropy Condition

Various versions of “the” entropy condition are known (cf. §3.8 of [9]), but the following is adequate for our purposes and indeed for any needs of traffic-flow theory that we can envisage. Let $k = k(x, t)$ be a weak solution of (2.1)-(2.3) that is continuous, except possibly for jump discontinuities along certain curves (*shocks*) $x = x_s(t)$ in the (x, t) -plane. It follows from the weak form (2.6) of the conservation law that the Rankine-Hugoniot jump condition

$$x'_s(t)[k(x_s(t)+, t) - k(x_s(t)-, t)] = [q(k(x_s(t)+, t)) - q(k(x_s(t)-, t))] \quad (3.1)$$

must hold along the shock. (Here $k(x_s(t)+, t)$ denotes the concentration just downstream of the shock at time t and $k(x_s(t)-, t)$ is that just upstream of it.) The entropy condition for such a shock is that the shock speed x'_s be restricted by the inequalities

$$q'(k(x_s(t)+, t)) > x'_s(t) > q'(k(x_s(t)-, t)). \quad (3.2)$$

(Thus kinematic waves downstream (upstream) of the shock have an algebraically larger (smaller) velocity than the shock itself; when plotted in the (x, t) plane, this means such waves followed backward in time must impinge on the shock, from both sides.)

It follows from known results (i.e., Theorem 4.4 of [7]) that (if q is concave) there exists at most one weak solution of the initial-value problem (2.1)-(2.3) that is continuous except for shocks, and that satisfies the entropy condition (3.2) along each such shock. In particular, note that the above entropy condition applied at any point along the stationary shock in the solution k_2 given by (2.10) would require that $v_f < 0 < -v_f$, which is patently untrue. Thus this condition would select k_1 (which has no shocks) from among the two contending weak solutions of the preceding paragraph, and it is the unique weak

solution satisfying the entropy condition. More generally, as $q'' < 0$, the entropy condition requires that the vehicular concentration increase as a shock is crossed in the downstream (increasing x) direction. (Ansorge [1] demonstrates, from the jump condition (3.1) and the mean-value theorem, that in fact this condition is, for a weak solution having only shocks as discontinuities, *equivalent* to the entropy condition (2.22).)

In order to provide a traffic-flow frame of reference for the description in the following section of the numerical method of Godunov, it is convenient to insert here a description of the two basic types of entropy-satisfying weak solutions of the Lighthill-Whitham model that correspond to a jump discontinuity in the initial data.¹ Consider first the case that $k_l > k_r$, where k_l (k_r) is the concentration just to the left (right), or upstream (downstream), side of the initial discontinuity. In this case the entropy condition does not permit a shock to develop, so the solution must be continuous for all $t > t_0$, where t_0 is the initial time. The solution in fact takes the form of a *wave fan*, in which a plot of the characteristics in the (x, t) plane would show a “fan” of characteristic lines (2.5) emerging from (x_0, t_0) (x_0 = location of initial discontinuity), with the rightmost characteristic having wave velocity $q'(k_r)$, the leftmost having wave velocity $q'(k_l)$, and the wave velocities varying continuously across the fan between these limits. If $q'(k_l) > 0$ ($q'(k_r) < 0$), then necessarily $q'(k_r) > 0$ ($q'(k_l) < 0$), therefore all wave velocities in the fan are positive (negative), and the wave fan propagates downstream (upstream). If $q'(k_l) < 0 < q'(k_r)$, then the leftmost waves fan out upstream, and the rightmost waves fan out downstream; we shall term this a *stationary wave fan*. (The solution k_2 given above contains an instance of such a wave fan.)

For reference in the following section, it is convenient here to note, for each of the three types of wave fans, what the concentrations and corresponding flows are at the initial location x_0 of the discontinuity and times immediately following t_0 . In the case of a wave fan propagating downstream (upstream), the subject concentration is $k^* = k_r$ (k_l), and the flow is $q^* = q(k^*) = q(k_r)$ (respectively, $= q(k_l)$). In the case of a stationary wave fan, the characteristic through x_0 at all $t > t_0$ corresponds to zero wave velocity, $q'(k^*) = 0$. But this implies $k^* = k_m$ and $q^* = q_m = q(k_m)$, where q_m is the capacity flow (i.e., maximum flow) for the particular fundamental diagram being used, and k_m is the concentration at this capacity flow. Note that, for all three types of wave forms, we can conveniently express q^* as

$$q^* = \max_{k_r \leq k \leq k_l} q(k). \quad (3.3)$$

¹In mathematical terms – cf. [9] – we are describing the solutions of the *Riemann problem* for the Lighthill-Whitham model that also satisfy the entropy condition.

Now consider the situation that $k_l < k_r$. In this case a shock develops, and it propagates upstream or downstream according respectively as the Rankine-Hugoniot shock velocity $[q(k_r) - q(k_l)]/(k_r - k_l)$ is respectively positive or negative. Such a shock describes the situation at the upstream extreme of a traffic jam, as already clearly elucidated by Lighthill and Whitham [8]. Note that if the shock moves downstream (upstream), then the concentration and flow at location x_0 and times immediately following t_0 are respectively $k^* = k_l$ (k_r) and $q^* = q(k^*) = q(k_l)$ (respectively, $q(k_r)$). Similarly to (3.3), this flow can be conveniently expressed as

$$q^* = \max_{k_l \leq k \leq k_r} q(k). \quad (3.4)$$

Given that the entropy condition (3.2) selects the unique weak solution for the initial-value problem (2.1)-(2.3) that is appropriate for traffic flow, why is this the case? That is, what is the significance within traffic-flow theory of the entropy condition? LeVeque (§3.8 of [9]) motivates the entropy condition as “required to pick out the physically relevant vanishing viscosity solution” (p. 36 of [9]). In the case of gas dynamics this is eminently reasonable, as it is well-known (i.e., Chap. 1 of [9]) that the Euler equations, which display shocks, are approximations to the Navier-Stokes equations, which contain viscosity and do not admit solutions containing shocks. In fact there is a well-developed body of literature (e.g., [3]) devoted to the development of such macroscopic flow equations from arguably more fundamental microscopic models of gases (i.e., the Boltzmann equation). In one such line of development, the Chapman-Enskog expansion (cf. §V.3 of [3]), the Euler equations appear as the lowest order formal macroscopic approximation and the Navier-Stokes equations as the next higher order such approximation. The advantage of such microscopically based derivations, as contrasted to those based strictly upon macroscopic considerations, is that the former also provide an “equation of state” (gas dynamic analog of the fundamental diagram of traffic-flow theory) and expressions for the coefficients that appear in the Navier-Stokes equations (i.e., viscosity and diffusion coefficient) in terms of microscopic models of molecular properties.

Some traffic-theoretic counterparts of these results from the field of gas dynamics exist, but on balance they are decidedly more sketchy. Ansonge interprets the entropy condition as asserting that drivers “try to smooth a discontinuous situation to a continuous one ... or not to decrease the density if they cross a discontinuity,” and he further describes the latter tendency to ride into a jam as “driver’s ride impulse” (p. 140 of [1]). It seems a reasonable assumption that the Lighthill-Whitham model is a traffic-theoretic analog of the Euler equations, although we are not aware of any development of these via a microscopic

(“kinetic”) viewpoint that is analogous to the Chapman-Enskog expansion cited in the preceding paragraph. (Prigogine and Herman (Chap. 5 of [13]) have given, in the context of their relaxation-time kinetic model, results that have elements of similarity to such a development, but they focus more upon the issue of solutions of the linearized kinetic equation that validate the kinematic wave solutions found by Lighthill and Whitham rather than upon development of the Lighthill-Whitham model *per se*.) A number of workers have given so-called higher-order approximations that seem candidates to be analogs of the Navier-Stokes equations. (See Kühne [6], Payne [11,12] and Ross [15]; see also Ross [16] for an excellent summary and review of such models.) In many instances the Lighthill-Whitham model is some obvious limiting form of these, but we are unaware of any effort to establish that the entropy condition for the Lighthill-Whitham model singles out the corresponding limit of the solution of a higher-order model. Further, we are unaware of any development of such a model as a “higher-order” approximation to the solution of some underlying kinetic model.² Finally, we note that Newell [10] has recently suggested an alternative for singling out the traffic-theoretically “correct” weak solution, namely as the lower envelope of all such solutions when the dependent variable is taken as the *cumulative* flow. It would be of some interest to determine if this in fact is equivalent to the entropy condition discussed here.

In the remainder of this note we set aside these issues of the traffic-theoretic basis for the entropy condition, but rather assume that it does select the desired solution and focus upon issues relating to numerical realization of the entropy condition. It is, as emphasized by LeVeque (p. 37 of [9]), a nontrivial task to implement the entropy condition numerically because of the difficulty in distinguishing between a discrete approximation to a shock that violates the entropy condition and such an approximation to a wave fan (as in k_2 above).

²As regards the meaning of present such models from the kinetic viewpoint, the situation has changed little from 20 years past, when Prigogine and Herman stated that “the physical meaning of such an extension is not clear” (p. 16 of Ref. 13).

Chapter 4

A Numerical Realization of the Entropy Condition: Godunov's Method

The method of Godunov is perhaps the most straightforward and simplest numerical scheme for scalar conservation laws that incorporates the entropy condition. This method is based on the use of characteristic information within the framework of a discrete counterpart of the conservation law. The following description of this method is largely based upon Chapters 13 and 14 of [9], as adapted to the Lighthill-Whitham model by means of the special entropy-satisfying solutions corresponding to jump discontinuities in initial data that were described in the preceding section.

As before, we consider the Lighthill-Whitham model

$$\frac{\partial k(x, t)}{\partial t} + \frac{\partial q(k(x, t))}{\partial x} = 0, \forall x \in I, t \geq 0, \quad (4.1)$$

where now the fundamental diagram (2.3) is explicitly incorporated into the conservation law. The basic form of the approximation produced by the method is simply that at each discrete time line, say $t = t_n$, the concentration $k(x, t_n)$ on each section, say $x_{j-1/2} < x < x_{j+1/2}$, is approximated by a constant, say K_j^n . It is convenient to think of K_j^n as an approximation to the spatial average of the true concentration over the subject section at the time line under consideration,

$$K_j^n \approx \frac{1}{h_j} \int_{x_{j-1/2}}^{x_{j+1/2}} k(x, t_n) dx, \quad (4.2)$$

where $h_j = x_{j+1/2} - x_{j-1/2}$. If we integrate the conservation law (4.1) over the region

$\{(x, t) : x_{j-1/2} < x < x_{j+1/2}, t_n < t < t_{n+1}\}$, then there results

$$\int_{x_{j-1/2}}^{x_{j+1/2}} k(x, t_{n+1}) dx = \int_{x_{j-1/2}}^{x_{j+1/2}} k(x, t_n) dx + \int_{t_n}^{t_{n+1}} q(k(x_{j-1/2}, t)) dt - \int_{t_n}^{t_{n+1}} q(k(x_{j+1/2}, t)) dt. \quad (4.3)$$

We shall require the K_j^n to satisfy a discrete counterpart of this integral conservation law, namely

$$K_j^{n+1} = K_j^n - \frac{\Delta t_n}{h_j} [Q(K_j^n, K_{j+1}^n) - Q(K_{j-1}^n, K_j^n)], \quad (4.4)$$

where Δt_n is the length of the time step and Q is a numerical approximation to the average flow past the section boundary $x_{j+1/2}$ during the time interval $[t_n, t_{n+1}]$,

$$Q(K_j^n, K_{j+1}^n) \approx \frac{1}{\Delta t_n} \int_{t_n}^{t_{n+1}} q(k(x_{j+1/2}, t)) dt. \quad (4.5)$$

Any numerical approximation of the form (4.4) is said to be *conservative*. Note that *any* conservative approximation is an explicit discrete approximation to (4.1), in that if the approximate section-average concentrations are given at any time line, then (4.4) is an explicit expression for the corresponding approximations at the next time line.

The particular form of the average flow function for Godunov's method can be simply described in terms of the previous description of the basic nature of the approximation produced by the method and the results of the preceding section. Let k_l (k_r) be the (approximate) constant concentration (at time t_n) just to the left (right) of the section boundary where it is desired to approximate the average flow during the next time step. That approximation is then taken as the (entropy-satisfying) flow at the section boundary immediately following time t_n that would correspond to these concentrations. From (3.3) and (3.4) this can be conveniently expressed as

$$Q(k_l, k_r) = q(k^*) = \begin{cases} \min_{k_l \leq k \leq k_r} q(k) & \text{if } k_l \leq k_r, \\ \max_{k_r \leq k \leq k_l} q(k) & \text{if } k_l > k_r. \end{cases} \quad (4.6)$$

Equation (4.6) is equivalent to the four relations

1. $q'(k_l), q'(k_r) \geq 0 \Rightarrow k^* = k_l$,
2. $q'(k_l), q'(k_r) \leq 0 \Rightarrow k^* = k_r$,
3. $q'(k_l) \geq 0 \geq q'(k_r) \Rightarrow k^* = \begin{cases} k_l & \text{if } [q]/[k] > 0 \\ k_r & \text{if } [q]/[k] < 0 \end{cases}$, and
4. $q'(k_l) < 0 < q'(k_r) \Rightarrow k^* = k_m$,

where $[q]/[k] = (q(k_r) - q(k_l))/(k_r - k_l)$, and k_m is the intermediate value satisfying

$$q'(k_m) = 0, \quad (4.7)$$

which is to say that it is the concentration corresponding to capacity flow. Case 1 corresponds to either a wave fan or a shock wave, according respectively as $q(k_r) - q(k_l)$ is negative or positive but moving downstream in either case. Similarly, case 2 corresponds to either a wave fan or a shock wave that is propagating upstream. Case 3 corresponds to a shock wave that is propagating downstream or upstream, according respectively as $q(k_r) - q(k_l)$ is positive or negative, while the fourth case is that of a stationary wave fan. The latter is the counterpart of a transonic rarefaction in gas dynamics. In this case, k^* equals k_m , which is the value where the characteristic speed is zero. In traffic-flow theory, this is the case of the dissolution of a traffic jam (i.e., traffic-signal release). Condition (4.7) says that the flow into the first post-signal section (after $t = 0$) in the first time increment is the capacity flow (i.e., the maximum value of the traffic flux). For the linear Greenshields' model, this is precisely the flow at half the jam concentration.

Chapter 5

Numerical Results for Simple Problems: Dissipation of Jams

The illustrative computations of this section were carried out with a dimensionless form of the simple Lighthill-Whitham model that was given in Chapter 2 (i.e., Equations (2.1)–(2.3)). To simplify the problem, the *fundamental diagram condition* (eq. (2.3)) was assumed to follow the Greenshields' Model (i.e., linear speed-density relationship, as in (2.7)).

Suppose $x \in I$ and $t \in [0, T]$, for an arbitrary finite time $T > 0$. These correlate to the observed freeway segment and observed time interval. We define the dimensionless variables

$$\tilde{k}(x, t) = \frac{k(x, t)}{k_j}, \quad \tilde{t} = \frac{t}{T}, \quad \tilde{x} = \frac{x}{v_f T},$$

where k_j and v_f are the corresponding maximum (traffic jam) density and maximum (freeflow) speed, respectively. If (2.1), (2.2) and (2.7) are multiplied by T and then are divided by k_j , the problem (2.1), (2.2), and (2.7) (with $g(x, t) = 0$) becomes

$$\frac{\partial \tilde{k}}{\partial \tilde{t}} + \frac{\partial \tilde{q}}{\partial \tilde{x}} = 0, \quad \forall \tilde{x} \in \tilde{I}, \tilde{t} \geq 0, \quad (5.1)$$

where $\tilde{k} = \tilde{k}(\tilde{x}, \tilde{t})$ is the dimensionless traffic density and $\tilde{q} = \tilde{q}(\tilde{k})$ is the dimensionless traffic flow rate satisfying

$$\tilde{q}(\tilde{k}) = (1 - \tilde{k})\tilde{k}. \quad (5.2)$$

The corresponding initial conditions are

$$\tilde{k}(\tilde{x}, 0) = \tilde{k}_0(\tilde{x}) = k_0(v_f T \tilde{x})/k_j, \quad \tilde{x} \in \tilde{I}. \quad (5.3)$$

Here, \tilde{I} is the modified freeway segment.

For our first numerical example, we take the problem of traffic-signal release with the initial condition

$$\tilde{k}_0(\tilde{x}) = \begin{cases} 1, & \text{for } \tilde{x} < 0.5 \\ 0, & \text{for } \tilde{x} \geq 0.5. \end{cases} \quad (5.4)$$

The modified freeway segment \tilde{I} is taken to be the interval $[0, 1]$. Figure 1a presents the results of the problem (5.1), (5.2), and (5.4) for 20 time steps with $\Delta t = 0.01$ and $\Delta x = 0.02$. The results for three different numerical methods (Godunov, upwind, and Lax-Friedrichs) are plotted against the exact solution, as adapted from k_1 of §2. Notice that the upwind method converges to the wrong weak solution (i.e., that given by k_2 of §2). This is surely due to the fact that the upwind method (even though it is a conservative method) does not satisfy the entropy condition. On the other hand, the Lax-Friedrichs method does satisfy the entropy condition but is generally excessively dissipative, which is to say it has a tendency of over smoothing its approximate solution. In fact, in this example it obviously overestimates the rate of propagation of both the leading and trailing characteristics of the wave fan. Godunov's method clearly produces somewhat more accurate approximations than the other two, even though both it and the Lax-Friedrichs method are known to converge (in the fine-mesh limit) to the correct weak solution (i.e., the stationary wave fan). The reader again is referred to [9], esp. Chaps. 10–18, for further details regarding these three methods.

Our second simple numerical experiment is the problem of release of a traffic platoon that is initially constrained, say by a slowly moving lead vehicle. The initial conditions for this problem are

$$\tilde{k}_0(\tilde{x}) = \begin{cases} 0.7, & \text{for } \tilde{x} < 0.5 \\ 0, & \text{for } \tilde{x} \geq 0.5. \end{cases} \quad (5.5)$$

The exact solution is

$$\tilde{k}_0(\tilde{x}, \tilde{t}) = \begin{cases} 0.7, & \text{for } \tilde{x} < 0.5 - 0.4\tilde{t} \\ \frac{(\tilde{t} - \tilde{x} + 0.5)}{2\tilde{t}}, & \text{for } 0.5 - 0.4\tilde{t} \leq \tilde{x} < 0.5 + \tilde{t} \\ 0, & \text{for } \tilde{x} \geq \tilde{t} + 0.5. \end{cases} \quad (5.6)$$

Again, a numerical simulation of 20 time steps is taken with $\Delta t = 0.01$ and $\Delta x = 0.02$. Figure 1b gives the numerical results of problem (5.1), (5.2), and (5.5), in comparison with the above exact solution. It can be seen that little change occurs for the Lax-Friedrichs and Godunov methods. However, now some jam dissipation is observed from the upwind method. Nonetheless, the amount of dissipation remains substantially less than the other two methods. Again the Lax-Friedrichs method is excessively dissipative. As a result,

Godunov's method still appears to be much superior to the other two numerical methods. Figure 2 compares the predicted traffic jam dissolution via Godunov's method (i.e., the numerical solution to problem (5.1), (5.2), and (5.4)) versus the preceding exact solution for various elapsed times.

Chapter 6

Numerical Results for Simple Problems: Formation of Jams

Even though our previous numerical simulations on the Lighthill-Whitham model using Godunov's method give somewhat realistic behavior of a traffic jam dissolution, questions still surface surrounding the accuracy of such a model relative to the widely used "higher-order" continuum models (e.g., Payne [11,12], Ross [15]). To explore this issue, we have chosen FREFLO, a macroscopic freeway traffic simulation code that was developed by Payne [11,12] to simulate a wide range of freeway conditions, as a basis for comparison. These comparisons have been effected for scenarios involving formation of traffic jams, as FREFLO is known to have difficulties in such settings; Rathi et al. [14] have recently modified FREFLO, using flow restrictions at the congested links, in an effort to simulate realistically congested flow conditions.

The FREFLO code is specifically based on Payne's model [11,12]), but it also contains extensions (from its predecessor MACK) that remove the restriction of a single linear traffic segment and distinguish between the different vehicle types (e.g., buses, carpools, trucks). Payne's model consists of the continuity equation (2.1), along with the "dynamic equation"

$$\frac{\partial v}{\partial t} + v \frac{\partial v}{\partial x} = \frac{[v_e(k) - v]}{c} - \left(\frac{b}{k}\right) \frac{\partial k}{\partial x}, \quad (6.1)$$

which can be considered as a replacement for the "static" fundamental diagram (2.3). Here

$v_e(k)$ = equilibrium speed-density relation,

c = relaxation (time) coefficient,

b = anticipation coefficient,

and the remaining notation is as previously. This equation models the mean acceleration of traffic as being comprised (linearly) of two components, a relaxation to some "equilibrium"

speed-density, and an anticipation term that is proportional to the logarithmic spatial derivative of the concentration.

Together with the conservation law (2.1), the initial conditions (2.2), and suitable boundary conditions, the dynamic equation (6.1) describes the dynamic traffic system of a freeway network. The corresponding discrete approximation to this model that is used in FREFLO is

$$K_j^{n+1} = K_j^n + \frac{\Delta t_n}{l_j h_j} [q_{j-1}^n - q_j^n + g_j^{on,n} - g_j^{off,n}], \quad (6.2)$$

and

$$v_j^{n+1} = v_j^n + \Delta t \left[-v_j^n \frac{(v_j^n - v_{j-1}^n)}{\Delta x_j} - \frac{1}{c_j} (v_j^n - v_e(K_j^n)) + \left(\frac{b_j}{K_j^n} \right) \frac{(K_{j+1}^n - K_j^n)}{\Delta x_j} \right], \quad (6.3)$$

where l_j is the number of lanes in section j , and otherwise the notation is similar to that used in the preceding two sections (except that K_j^n now is an approximation to the density *per lane*, averaged over section j). Given values for the source terms (i.e., the $g_j^{on,n}$ and $g_j^{off,n}$), the equilibrium speed density relation, the relaxation time coefficient and the anticipation coefficient, these equations can be explicitly solved for the approximate concentrations and mean speeds. For all of our numerical simulations it is assumed that no vehicles enter or leave the freeway (i.e., $g_j^{on,n} = g_j^{off,n} = 0$). For the equilibrium speed-density relation we used the default value for the version of FREFLO that was used [5]

$$v_e(k) = c_1 + c_2(k \times 10^{-2}) + c_3(k \times 10^{-2})^2 + c_4(k \times 10^{-2})^3 \quad \text{miles per hour}, \quad (6.4)$$

with $c_1 = 107$, $c_2 = -231$, $c_3 = 215$, and $c_4 = -74$ and a cutoff at a maximum speed of 55 mph. (This relationship is displayed graphically in Figure 3.) Similarly the default values of 75 seconds per mile and .25 miles²/hour were used for respectively the relaxation time coefficient and the anticipation coefficient. Apparently [14] the boundary conditions used in FREFLO correspond to a “false boundary” implementation of the condition $\frac{\partial v}{\partial x} = 0$ at the upstream boundary of the freeway segment under consideration and $\frac{\partial k}{\partial x} = 0$ at the downstream boundary; the traffic-theoretic significance of these conditions does not seem clear.

Modeling of incidents by FREFLO can be accomplished by the specification of a reduction in the number of available lanes, a constraint on the flow rate past the incident site, or an alteration to the relaxation and anticipation coefficients. We simulated two different scenarios with FREFLO, to compare with Godunov’s method applied to the Lighthill-Whitham model. Since the Lighthill-Whitham model can only model one-lane traffic, we considered, for both scenarios, a one-lane freeway test with total roadway length of 1 mile.

For both the Godunov approximation to the Lighthill-Whitham model and FREFLO, a uniform spatial mesh with sections of width 0.1 mile was employed. The speed-density relation of Figure 3 was employed as the fundamental diagram for the Lighthill-Whitham model and as the equilibrium speed-density relation for FREFLO. The corresponding freeflow speed and equilibrium capacity flow ($:= \max_k \{k v_e(k)\}$) are respectively $v_f = 55$ miles per hour (mph) and $q_m = 3000$ vehicles per hour (vph). (The corresponding density at capacity flow is approximately 50.66 vehicles per lane-mile.) These relations were assumed to hold uniformly in space, except at the midpoint of the section under consideration (i.e., $x = 0.5$ miles), where a lower capacity flow constraint (bottleneck) was specified. This corresponds to a road segment where some flow-restricting incidents have occurred. For Godunov's method the flow at the inlet to the bottleneck section was specified as the minimum of the normal flow and an upper limit that will be described below for the individual scenarios. For the FREFLO calculations a uniform nominal capacity (a required input to FREFLO for each section) of 3000 vph throughout the roadway was specified, except at the bottleneck, where an incident was specified, with input flow limited as will be described for the individual scenarios.

For both scenarios and methods the calculations were effected over an observable time interval of 4 mins. and 12 secs. For FREFLO uniform time steps of 4 secs. were employed, while the method of Godunov used steps of 4.5 secs. For both methods and scenarios it was assumed that no traffic was present on the observable freeway at time $t = 0$ (i.e., $k_0 \equiv 0$). The only difference between the two scenarios was thus the flow assumed at the section entrance and the magnitude of the flow restriction at the midpoint of the test section.

For the first scenario an entry flow of 1400 vph was taken at the entry point of the section, $x = 0$. The freeway bottleneck was implemented at $x = 0.5$ miles with a restricted flow of 700 vph. Thus the entry flow was well below the "normal" capacity flow of 2000 vph but well above the bottleneck capacity. We therefore expect the Lighthill-Whitham solution first to display a wave fan propagating downstream from the section entry. This indeed is shown by Godunov's method, per the curve in Fig. 4 labeled 0 mins. 36 secs. However, once the wave (characteristic) corresponding to the bottleneck capacity on the fundamental diagram (i.e., Fig. 3) reaches the bottleneck, a backward propagating shock begins to form at the bottleneck. This in fact happens fairly early, as the concentration required upstream of the bottleneck to initiate shock formation is only about half ($k_b \approx 12.73$ vph) that of the inlet concentration (≈ 25.5 vph). (Throughout the figures the concentration at the inlet is plotted as that at $x = 0.1$ miles, to avoid distracting and

insignificant graphical effects near the inlet.) Indeed Godunov's method (cf. Fig. 4) shows the shock beginning to form at $t = 1$ min. 12 secs. and quite well-developed at $t = 1$ min. 48 secs. For the Godunov approximation to the Lighthill-Whitham model (Fig. 4) the jam develops smoothly, with a concentration upstream of the bottleneck slightly below jam density ($k_j = 142.5$ vehicles per mile (vpm)) propagating rather slowly backward from the site of the incident. After an initial transient, flow downstream of the bottleneck holds steady at the concentration $k_b \approx 12.73$ vpm corresponding to bottleneck capacity.

By contrast, while the corresponding FREFLO results (cf. Fig. 5) initially show the concentration rising smoothly upstream of the bottleneck, these seem to become somewhat erratic after two or three minutes, and by four minutes these concentrations even are decreasing, which is decidedly counterintuitive. After about two minutes the flow downstream of the bottleneck seems to display some oscillations. It is conceivable that these are related to the start-stop waves discussed by Kühne [6], although a definitive connection would seem to require further analysis.

The second test scenario incorporates an entry volume of 2000 vph and a bottleneck capacity of 1000 vph. The inflow at the entry section is slightly greater than the capacity flow (1925 vph) for the test section. Thus for the Lighthill-Whitham model a stationary wave fan immediately forms at the entry point. This is readily seen in the results for the method of Godunov applied to this model (Figure 6), especially at earlier times. When the wave (characteristic) having concentration k_b corresponding to flow = 1000 vph arrives at the bottleneck, a backward-propagating shock forms there. This concentration is slightly higher than that in the first scenario, so that the backward-propagating shock now is somewhat slower developing. However, the major difference is that now the densities between the entry section and the bottleneck also increase because of the effect of the stationary wave fan emanating from the entry point at $t = 0$. Again, the flow is essentially constant (at the bottleneck capacity) downstream of the bottleneck, following an initial transient.

Figure 7 shows the corresponding results obtained from FREFLO. As in previous scenarios, the concentrations upstream of the bottleneck appear somewhat erratic and difficult to explain, perhaps even more so because now there are oscillations there as well as downstream of the incident. Furthermore, unrealistically high densities can be seen from Figure 7. Traffic density reaches as high as 175 vehicles per lane-mile, which is considerably higher than normally observed values of about 100–120 vehicles per lane-mile on a congested freeway (see Rathi [14]).

For the two above scenarios, Tables 1 and 2 provide the corresponding numerical results for Godunov's approximation to the Lighthill-Whitham model, as presented in Figures 4 and 6, while Tables 3 and 7 give the corresponding numerical results for FREFLO as presented in Figures 5 and 7. In addition, corresponding FREFLO velocities and flows for the two scenarios are given in Tables 4-6 and 8-10.

Chapter 7

Conclusions

The basic purpose of this work was to investigate the possibility that previously reported difficulties in simulating congested flow could be reduced by the use of numerical approximations that satisfy a so-called “entropy condition.” This was done by applying the simplest such approximation (Godunov’s method) to the conceptually simple and classical Lighthill-Whitham conservation model of traffic flow, and by comparing the results to those obtained from similar situations by means of the widely used FREFLO code. While the two approaches by no means produce identical results, it is not clearly the case that either approach is superior. It is somewhat surprising that the Lighthill-Whitham model performs reasonably in simulating formation and dissolution of traffic jams, especially in view of earlier reports of unsatisfactory results from this model. It appears conceivable that such reports might, at least in part, be due to use of numerical approximations that do not satisfy the entropy condition, rather than to a defect in the model itself.

Future related research will be centered around two tasks:

- i. continued study of the behavior of Godunov’s method for the single-lane Lighthill-Whitham model, especially at the entrance into traffic jams;
- ii. either initiation of implementation of this method into a realistic computer code (e.g., multilane models), if warranted by the results of the preceding task, or identification and preliminary exploration of alternate numerical methods that satisfy entropy conditions, if the results of task i suggest that Godunov’s method is inadequate.

The ultimate significance of this work is envisioned to be in implementation of the entropy condition in a computer code to analyze existing vehicular traffic conditions and to predict future scenarios in Texas (and elsewhere). With current computational capabilities,

only continuum models of traffic flow realistically provide the ability to model traffic flow on large scales (in either space or time). Currently such models do not perform adequately in congested traffic conditions, which are precisely the conditions of paramount current interest in studies relating to efficient use of fuel and minimization of vehicular pollution in urban settings. We believe the effort reported here offers great promise in overcoming existing limitations and thus providing a substantially improved tool for modeling a variety of problems that are important to the continued development of the ability to meet transportation needs.

Acknowledgments

The authors would like to express their gratitude to Dr. Thomas Urbanik II, of the Texas Transportation Institute, and Dr. Ray Krammes, of the Division of Civil Engineering of the Texas Engineering Experiment Station, for many suggestions during the course of this investigation. This work was also supported in part by the Texas Transportation Institute. The Texas Transportation Institute and the Texas Engineering Experiment Station are components of the Texas A&M University System.

References

1. R. Ansorge, "What Does the Entropy Condition Mean in Traffic Flow Theory?," *Transpn. Res. B*, **24B**(1990), 133-144.
2. P. S. Babcock, IV, D. M. Auslander, M. Tomizuka, and A. D. May, "Role of Adaptive Discretization in a Freeway Simulation Model," *Transp. Res. Rec.*, **971**(1984), 80-92.
3. Carlo Cercignani, *The Boltzmann Equation and its Applications*, Springer-Verlag, New York, 1988.
4. B. D. Greenshields, "A Study of Traffic Capacity," *Proc. Highway Research Board*, **14**(1934), 448-477.
5. FREFLO Version M 100.15, *Federal Highway Administration*, 1987.
6. R. Kühne, "Macroscopic Freeway Model for Dense Traffic – Stop-Start Waves and Incident Detection," *Ninth International Symposium on Transportation and Traffic Theory*, VNU Science Press, 1984, pp. 21-42.
7. P. D. Lax, *Hyperbolic Systems of Conservation Laws and The Mathematical Theory of Shock Waves*, Society for Industrial and Applied Mathematics, Philadelphia, 1974.
8. M. J. Lighthill, F.R.S. and G. B. Whitham, "On Kinematic Waves II. A Theory of Traffic Flow on Long Crowded Roads," *Proc. Royal Society, London*, **A229**(1955), 317-345.
9. R. J. LeVeque, *Numerical Methods for Conservation Laws*, Birkhäuser Verlag, Basel, Germany, 1990.
10. Gordon F. Newell, "A Simplified Theory of Kinematic Waves," Report No. UCB-ITS-RR-91-12, Institute of Transportation Studies, University of California at Berkeley, September 1991.
11. H. J. Payne, "FREFLO: A Macroscopic Simulation Model of Freeway Traffic," *Transp. Res. Rec.*, **722**(1979), 68-77.
12. H. J. Payne, "Discontinuity in Equilibrium Freeway Traffic Flow," *Transp. Res. Rec.*, **971**(1984), 140-145.

13. Ilya Prigogine and Robert Herman, *Kinetic Theory of Vehicular Traffic*, American Elsevier, New York, 1971.
14. A. K. Rathi, E. B. Lieberman, and M. Yedlin, "Enhanced FREFLO: Modeling of Congested Environments," *Transp. Res. Rec.*, **112**(1988), 61-71.
15. P. Ross, "Traffic Dynamics," *Transpn. Res. B*, **22B**(1988), 421-435.
16. P. Ross, "Some Properties of Macroscopic Traffic Models," preprint.

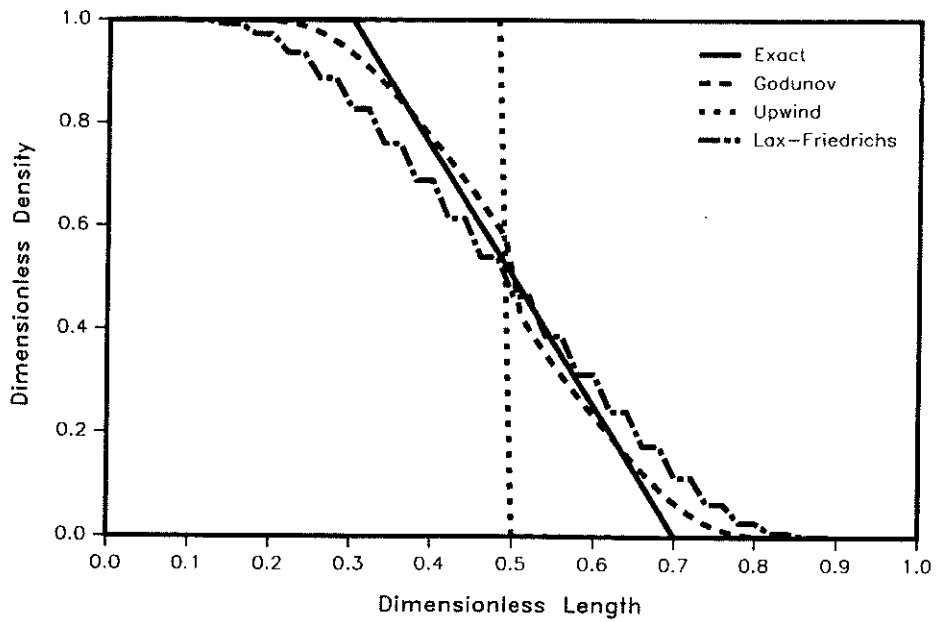


Figure 1a: The traffic-signal release: $\Delta t = 0.01$; $\Delta x = 0.02$; $t = 0.2$.

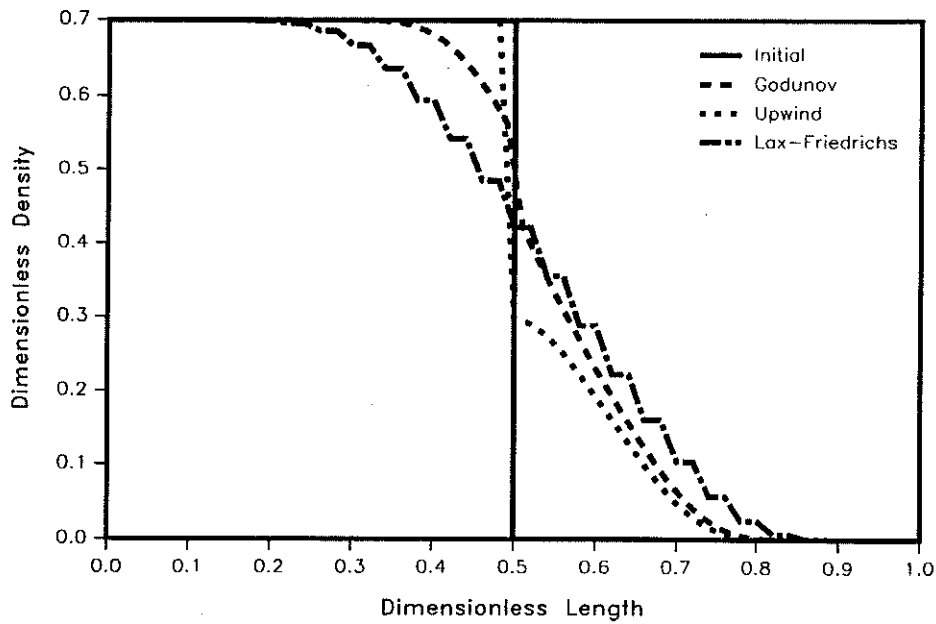


Figure 1b: The moderately congested signal release: $\Delta t = 0.01$; $\Delta x = 0.02$; $t = 0.2$.

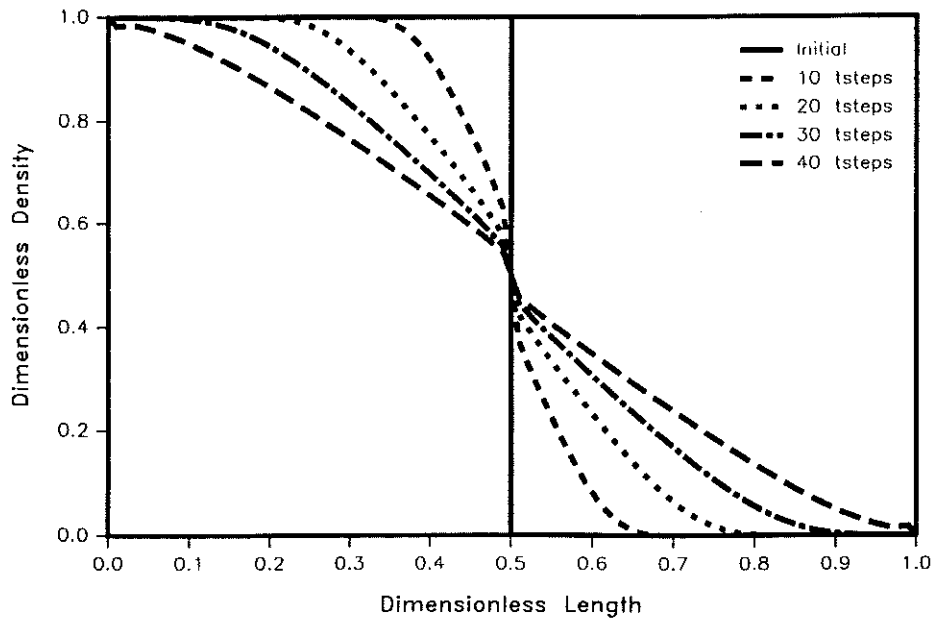


Figure 2: The traffic-signal release via Godunov's method: $\Delta t = 0.01$; $\Delta x = 0.02$.

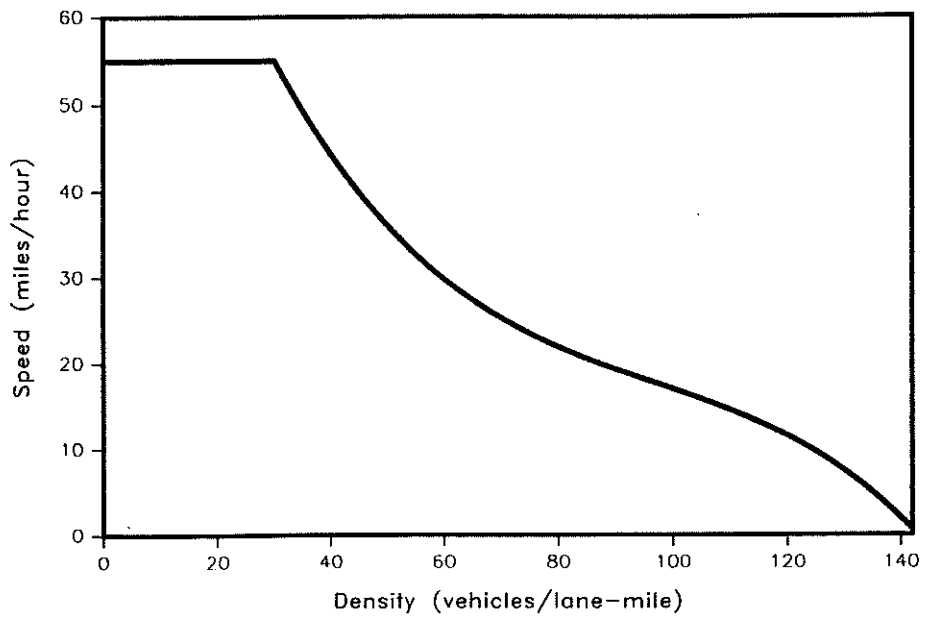


Figure 3: The speed-density relation.

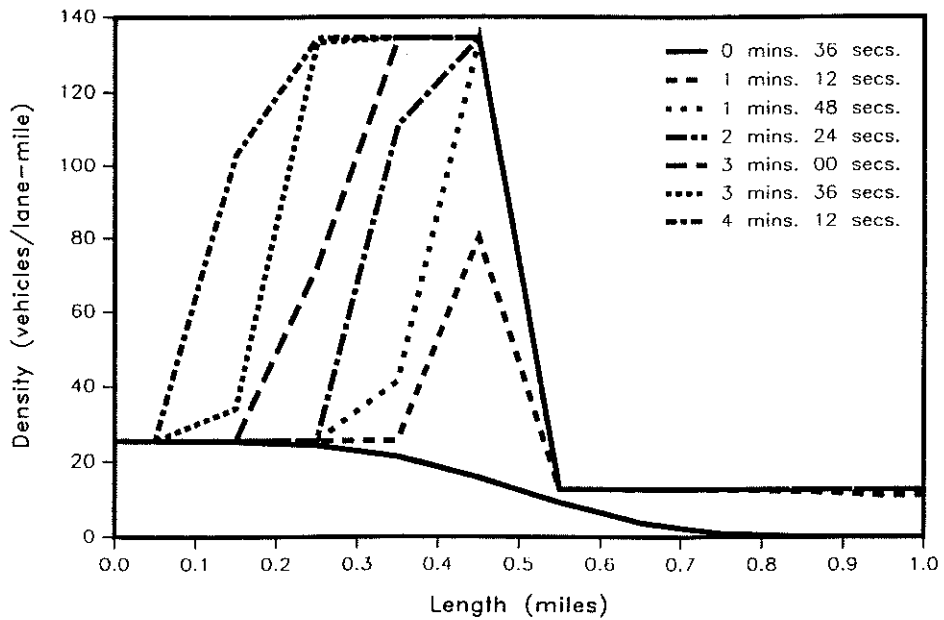


Figure 4: The freeway bottleneck via Godunov's method for scenario 1: $\Delta t = 3.6$ seconds; $\Delta x = 0.1$ miles; entry flow rate = 1400 vph; restricted flow rate = 700 vph.

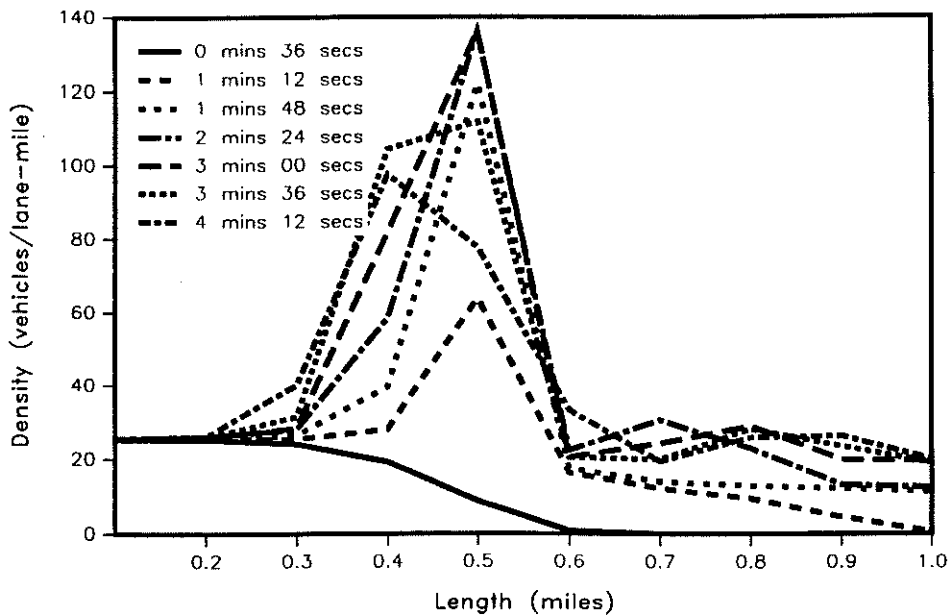


Figure 5: The freeway bottleneck via FREFLO for scenario 1: $\Delta t = 4.0$ seconds; $\Delta x = 0.1$ miles; entry flow rate = 1400 vph; restricted flow rate = 700 vph.

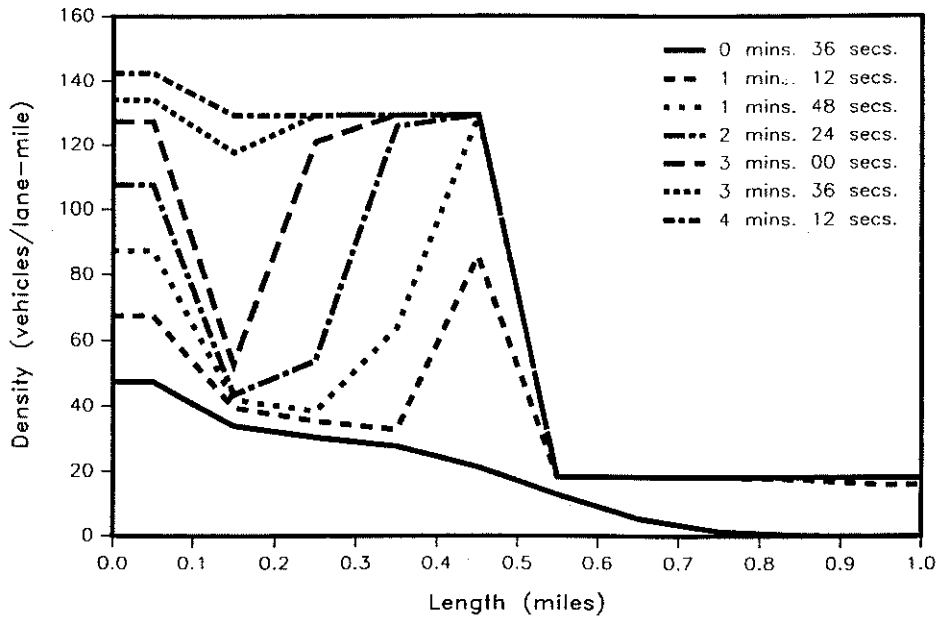


Figure 6: The freeway bottleneck via Godunov's method for scenario 2: $\Delta t = 3.6$ seconds; $\Delta x = 0.1$ miles; entry flow rate = 2000 vph; restricted flow rate = 1000 vph.

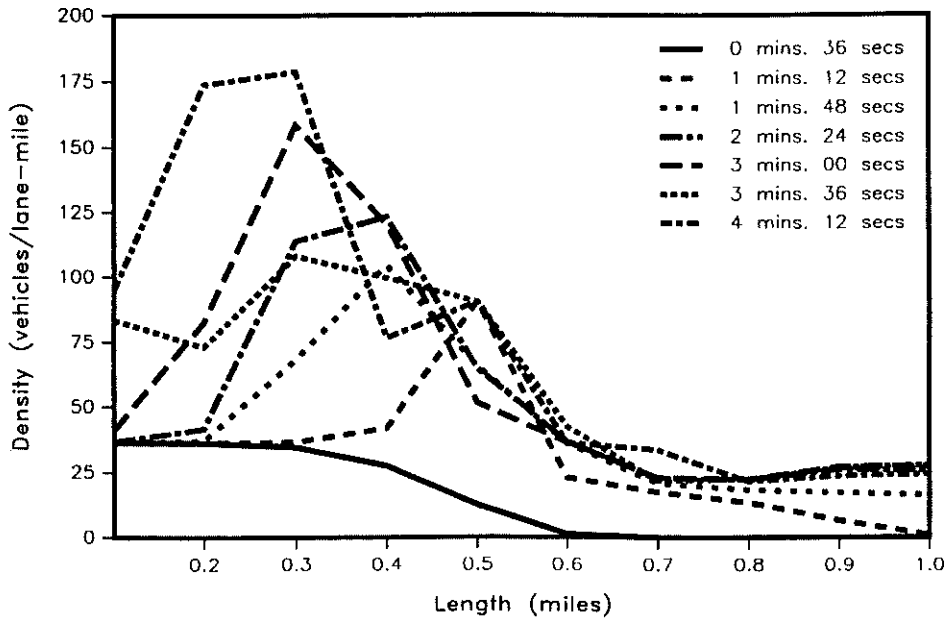


Figure 7: The freeway bottleneck via FREFLO for scenario 2: $\Delta t = 4.0$ seconds; $\Delta x = 0.1$ miles; entry flow rate = 2000 vph; restricted flow rate = 1000 vph.

Density (vehicles/lane-mile)											
Time (sec.)	Length (miles)										
	0.0	0.1	0.2	0.3	0.4	0.5	0.6	0.7	0.8	0.9	1.0
36	25.44	25.22	24.19	21.23	15.82	9.20	3.81	0.98	0.12	0	0
72	25.45	25.45	25.45	25.44	80.10	12.73	12.71	12.61	12.21	11.17	11.17
108	25.45	25.45	25.45	41.38	134.2	12.73	12.73	12.73	12.73	12.73	12.73
144	25.45	25.45	25.45	111.1	134.5	12.73	12.73	12.73	12.73	12.73	12.73
180	25.45	25.45	72.04	134.5	134.5	12.73	12.73	12.73	12.73	12.73	12.73
216	25.45	34.12	133.4	134.5	134.5	12.73	12.73	12.73	12.73	12.73	12.73
252	25.45	103.1	134.5	134.5	134.5	12.73	12.73	12.73	12.73	12.73	12.73

Table 1: Traffic densities obtained from Godunov's method for scenario 1. Entry flow rate = 1400 vph. Restricted flow rate = 700 vph at 0.5 miles.

Density (vehicles/lane-mile)											
Time (sec.)	Length (miles)										
	0.0	0.1	0.2	0.3	0.4	0.5	0.6	0.7	0.8	0.9	1.0
36	47.47	33.88	30.27	27.46	21.24	12.74	5.38	1.40	0.17	0	0
72	67.49	39.46	35.25	32.56	85.56	18.18	18.15	18.00	17.41	15.90	15.90
108	87.48	42.00	38.31	63.57	129.0	18.18	18.18	18.18	18.18	18.17	18.17
144	107.5	43.50	53.87	126.0	129.5	18.18	18.18	18.18	18.18	18.18	18.18
180	127.5	52.80	121.1	129.5	129.5	18.18	18.18	18.18	18.18	18.18	18.18
216	134.3	117.7	129.5	129.5	129.5	18.18	18.18	18.18	18.18	18.18	18.18
252	142.5	129.5	129.5	129.5	129.5	18.18	18.18	18.18	18.18	18.18	18.18

Table 2: Traffic densities obtained from Godunov's method for scenario 2. Entry flow rate = 2000 vph. Restricted flow rate = 1000 vph at 0.5 miles.

Density (vehicles/lane-mile)

Time (sec.)	Section									
	1	2	3	4	5	6	7	8	9	10
36	25.4	25.3	24.1	19.2	8.7	0.8	0	0	0	0
72	25.4	25.4	25.5	29.1	63.9	16.3	12.2	9.5	4.5	0.6
108	25.4	25.5	26.5	39.6	122.2	17.5	14.0	12.9	12.2	11.3
144	25.5	26.1	28.1	58.4	136.1	22.5	30.7	23.0	13.2	12.5
180	25.5	26.1	28.4	81.8	136.1	20.6	24.4	29.1	20.0	19.6
216	25.5	26.0	31.5	104.4	111.9	20.5	20.0	28.3	23.6	19.1
252	25.6	26.3	40.1	97.5	77.6	33.3	19.5	26.0	26.4	20.1
288	25.6	30.0	56.1	54.5	118.3	36.0	30.7	19.2	25.7	25.4
324	25.8	31.7	48.7	69.5	135.0	23.7	31.5	22.8	20.0	25.8
360	26.2	37.9	69.8	70.9	134.4	22.9	32.0	25.9	18.9	22.7

Table 3: Traffic densities obtained from FREFLO for scenario 1. Entry flow rate = 1400 vph. Restricted flow rate = 700 vph.

Speed (miles/hr)

Time (sec.)	Section									
	1	2	3	4	5	6	7	8	9	10
36	55	55	55	55	55	55	0	0	0	0
72	55	55	54.5	46.6	10.9	41.3	51.1	54.3	55.0	54.9
108	55	54.8	51.9	30.6	5.7	39.7	49.5	53.0	54.3	55.0
144	54.8	54.1	51.6	19.3	5.1	40.1	45.5	55.0	51.9	55.0
180	54.8	54.4	43.3	12.2	20.8	34.5	54.0	51.3	55.0	50.5
216	54.8	54.1	37.5	8.3	6.2	45.8	41.3	55.0	52.5	55.0
252	54.9	52.2	29.1	25.2	9.0	55.0	46.1	51.0	55.0	51.9
288	54.2	43.2	42.2	31.2	5.9	49.9	42.9	54.2	54.8	55.0
324	53.6	47.0	46.2	27.7	5.2	31.9	55.0	46.3	55.0	52.5
360	52.3	42.0	35.8	28.0	5.2	40.1	44.3	55.0	47.8	55.0

Table 4: Traffic speeds obtained from FREFLO for scenario 1. Entry flow rate = 1400 vph. Restricted flow rate = 700 vph.

In-flow (vph)

Time (sec.)	Section									
	1	2	3	4	5	6	7	8	9	10
36	1397	1397	1361	1177	626	76	0	0	0	0
72	1397	1397	1397	1397	1321	698	644	576	320	54
108	1397	1397	1393	1379	1238	698	698	688	673	634
144	1397	1393	1382	1577	1843	698	1699	1303	742	648
180	1397	1397	1408	1570	0	698	749	1728	1040	1022
216	1397	1397	1422	1462	0	691	918	1404	1411	889
252	1397	1397	1426	1141	958	691	846	1339	1483	1127
288	1397	1397	1249	940	2210	698	1832	889	1318	1480
324	1397	1393	1220	2243	2261	698	1418	1408	842	1393
360	1397	1386	1145	3028	2171	698	1782	1339	897	1091

Table 5: Traffic in-flow rates obtained from FREFLO for scenario 1. Entry flow rate = 1400 vph. Restricted flow rate = 700 vph.

Out-flow (vph)

Time (sec.)	Section									
	1	2	3	4	5	6	7	8	9	10
36	1397	1379	1271	868	245	0	0	0	0	0
72	1397	1397	1386	1318	698	666	587	432	137	7
108	1397	1386	1375	1228	698	695	695	677	655	594
144	1386	1404	1552	0	698	742	1667	950	702	655
180	1397	1411	1447	0	691	904	1400	1397	875	1148
216	1397	1418	1231	0	2833	698	1328	1472	1120	1019
252	1397	1379	1066	3071	2768	1523	907	1559	1242	1062
288	1397	1220	2592	2200	698	1383	1458	1094	1508	1274
324	1382	1300	2538	1912	698	1793	1325	897	1109	1451
360	1372	1202	2401	1627	698	749	1735	1062	1084	1339

Table 6: Traffic out-flow rates obtained from FREFLO for scenario 1. Entry flow rate = 1400 vph. Restricted flow rate = 700 vph.

Density (vehicles/lane-mile)

Time (sec.)	Section									
	1	2	3	4	5	6	7	8	9	10
36	36.3	36.2	34.6	27.5	12.4	1.3	0	0	0	0
72	36.3	36.3	36.6	41.9	90.6	23.0	17.5	13.5	6.6	1.0
108	36.4	37.1	68.2	104.4	65.6	36.0	20.9	18.4	17.3	16.3
144	36.6	41.6	113.9	123.2	64.7	36.8	22.9	22.4	26.3	26.0
180	41.0	82.5	158.5	120.5	51.4	36.5	23.1	22.6	27.4	27.7
216	83.5	73.0	108.1	99.5	90.4	42.5	21.9	22.5	27.0	28.0
252	95.0	173.8	178.7	76.6	90.4	36.3	33.7	21.6	23.8	24.4
288	71.8	108.8	154.0	90.9	75.5	43.5	28.6	21.6	23.0	27.7
324	92.5	68.7	136.4	116.4	55.8	36.6	22.3	22.0	24.7	28.6
360	47.5	99.2	153.9	127.8	52.2	36.5	23.0	22.5	27.0	27.7

Table 7: Traffic densities obtained from FREFLO for scenario 2. Entry flow rate = 2000 vph. Restricted flow rate = 1000 vph.

Speed (miles/hr)

Time (sec.)	Section									
	1	2	3	4	5	6	7	8	9	10
36	55.0	55.0	55.0	55.0	55.0	55.0	0	0	0	0
72	55	55	53.9	43.2	11.0	41.7	51.5	55.0	55.0	55.0
108	55	52.3	21.6	24.7	15.2	55.0	45.5	55.0	54.5	55.0
144	54.5	39	10.9	19.5	15.5	55.0	46.5	50.5	55.0	55.0
180	50.1	18.6	0	19.5	19.5	55.0	46.1	50.6	55.0	55.0
216	27.1	31.6	14	23.6	11.1	36.7	53.6	48.8	55.0	55.0
252	16.9	0	0	29.1	11.1	48.0	47.3	55.0	51.0	55.0
288	29.0	16.4	0	25.7	13.3	38.1	55.0	47.7	55.0	54.1
324	25.1	26.0	8.7	20.3	17.9	55.0	44.8	55.0	50.9	55.0
360	32.1	16.0	0.0	18.6	19.2	55.0	46.0	50.9	55.0	55.0

Table 8: Traffic speeds obtained from FREFLO for scenario 2. Entry flow rate = 2000 vph. Restricted flow rate = 1000 vph.

In-flow (vph)										
Time (sec.)	Section									
	1	2	3	4	5	6	7	8	9	10
36	1998	1998	1958	1685	893	112	0	0	0	0
72	1998	1998	1998	1987	1847	1001	936	817	472	79
108	1998	1998	1991	1606	1199	994	1159	983	961	914
144	1994	2002	1994	0	0	994	1170	1166	1346	1530
180	1937	2167	2606	0	0	994	1192	1163	1375	1606
216	4	2228	2308	0	1375	2732	1008	1152	1350	1624
252	2336	2797	0	0	2376	1001	2012	994	1238	1364
288	4	2614	0	0	2992	2639	1566	1166	1091	1480
324	4	2437	1980	0	0	994	1192	1044	1282	1602
360	4	2344	2524	0	0	994	1188	1152	1354	1613

Table 9: Traffic in-flow rates obtained from FREFLO for scenario 2. Entry flow rate = 2000 vph. Restricted flow rate = 1000 vph.

Out-flow (vph)										
Time (sec.)	Section									
	1	2	3	4	5	6	7	8	9	10
36	1998	1973	1822	1238	346	7	0	0	0	0
72	1998	1998	1973	1829	1001	954	846	626	191	18
108	1998	1951	0	3128	2632	1544	1066	968	932	860
144	1994	1692	0	2714	2671	1595	1116	1292	1555	1274
180	2095	0	4	2992	2628	1570	1145	1310	1595	1393
216	2441	2495	0	2473	1001	1202	1051	1278	1598	1415
252	0	0	0	2376	1004	1645	1613	1022	1408	1206
288	2304	0	0	2326	1001	2005	990	1210	1260	1580
324	2437	1519	0	2794	2642	1566	1166	1087	1472	1530
360	2196	0	0	2992	2628	1570	1134	1292	1602	1386

Table 10: Traffic out-flow rates obtained from FREFLO for scenario 2. Entry flow rate = 2000 vph. Restricted flow rate = 1000 vph.